

4-Oxo- β -lactams (Azetidine-2,4-diones) Are Potent and Selective Inhibitors of Human Leukocyte Elastase

Jalmira Mulchande,[†] Rudi Oliveira,[†] Marta Carrasco,[†] Luís Gouveia,[†] Rita C. Guedes,[†] Jim Iley,[‡] and Rui Moreira^{*†}

[†]*iMed.UL, Faculty of Pharmacy, University of Lisbon, Av. Prof. Gama Pinto, 1649-003 Lisbon, Portugal and* [‡]*Department of Chemistry and Analytical Sciences, The Open University, Milton Keynes, MK7 6AA, U.K.*

Received July 21, 2009

Human leukocyte elastase (HLE) is a serine protease stored in and secreted from neutrophils that plays a determinant role in the pathogenesis of several lung diseases. 4-Oxo- β -lactams, previously reported as acylating agents of porcine pancreatic elastase, were found to be selective and potent inhibitors of HLE. Structure–activity relationship analysis showed that inhibitory activity is very sensitive to the nature of C-3 substituents, with small alkyl substituents such as a gem-diethyl group improving the inhibitory potency when compared to gem-methyl benzyl or ethyl benzyl counterparts. 4-Oxo- β -lactams containing a heteroarylthiomethyl group on the para position of an *N*¹-aryl moiety afforded highly potent and selective inhibition of HLE, even at a very low inhibitor to enzyme ratio, as shown by the k_{on} value of $3.24 \times 10^6 \text{ M}^{-1} \text{ s}^{-1}$ for **6f**. The corresponding ortho isomers were 40- to 90-fold less potent.

Introduction

Chronic obstructive pulmonary disease (COPD^a) is a progressive and ultimately fatal chronic illness¹ that is one of the fastest growing causes of death worldwide.^{2–4} Active exposure to cigarette smoke is the cause of the vast majority of COPD cases in Europe and the U.S.^{1,5,6} Aside from smoking cessation and domiciliary oxygen therapy, all current treatment strategies for COPD are largely aimed at improving symptoms and reducing exacerbations. Thus, there is an urgent need to develop novel therapeutic strategies to slow the progression of COPD and to improve the management of COPD patients beyond that achieved by current therapies.⁷

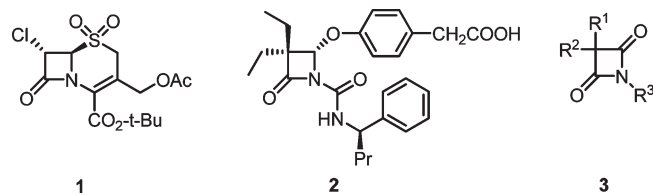
The inflammatory basis of COPD is complex, and it is known to involve the recruitment of macrophages, neutrophils, and CD8⁺ T cells into the lungs upon an inflammatory stimulus.^{1,6} Release of proteases from neutrophils is one of the several mechanisms involved in the pathogenesis of COPD. Human leukocyte elastase (HLE), along with proteinase 3 and cathepsin G, is a neutrophil serine protease member of the chymotrypsin superfamily, being expressed primarily in neutrophils and stored in their azurophilic granules.⁸ These neutrophil serine proteases are involved in pathogen killing within phagolysosomes, while extracellularly they degrade extracellular matrix proteins, such as elastin, collagen, laminin, fibronectin, and proteoglycans, and play an important role in the modulation of the inflammatory response.^{8,9} In particular, HLE is the most efficient neutrophil serine protease in the turnover of matrix proteins and, in addition, activates other proteases (e.g., metalloproteinases) and up-regulates inflammation.^{10–13} Unregulated activity of HLE during pulmonary inflammation,

which is a result of an imbalance between protease and its endogenous inhibitors (α_1 -antitrypsin and secretory leukoprotease inhibitor), leads to an excessive tissue destruction.¹¹ This protease/antiprotease imbalance appears to be a key pathogenic determinant in COPD as well in other inflammatory disorders such as acute respiratory distress syndrome (ARDS) and cystic fibrosis.^{14–17} Thus, HLE is an attractive target for therapeutic intervention, since selective inhibitors of this enzyme can reestablish the protease/antiprotease balance, which makes this a promising strategy for the treatment of COPD and other inflammatory disorders.^{18–20}

β -Lactams are well-known acylating agents of serine enzymes, including the bacterial transpeptidases and class A and class C β -lactamases.²¹ The first irreversible inhibitors of HLE based on the β -lactam scaffold were the cephalosporin sulfones derivatives, **1** (Chart 1).²² Molecular simplification of the β -lactam template led to the development of azetidine-2-ones, e.g., **2** (L-680,833), as potent, orally available, and hydrolytically more stable inhibitor of HLE.^{23–26} Increasing the intrinsic chemical reactivity of the β -lactam motif has been a strategy to increase the rate of acylation of the catalytic serine residue and improve inhibitory properties.^{27–31} We recently described the design rationale and some preliminary biochemical evaluation findings of a novel class of acylating agents, the 4-oxo- β -lactams (azetidine-2,4-diones), **3**.³² These compounds were found to be time dependent inhibitors of porcine pancreatic elastase, PPE, which shares ~40% homology and the catalytic triad with HLE.³³ The most potent PPE inhibitor also emerged as very potent inhibitor of the HLE.³² This promising result has prompted us to investigate the structure–activity relationships (SAR) of 4-oxo- β -lactams, **3**, toward the therapeutic target HLE. In this context, new compounds have been synthesized to explore the structural motifs at C-3 and N-1 of the 4-oxo- β -lactam scaffold required for optimal molecular recognition by HLE. These studies enable us to describe the mechanism of HLE inhibition and

*To whom correspondence should be addressed. Phone: +351 217946477. Fax: +351 217946470. E-mail: rmoreira@ff.ul.pt.

^aAbbreviations: HLE, human leukocyte elastase; COPD, chronic obstructive pulmonary disease; ARDS, acute respiratory distress syndrome; PPE, porcine pancreatic elastase.

Chart 1. Chemical Structures of Cephalosporin Sulfone, **1**, Azetidin-2-one, **2**, and 4-Oxo- β -lactams, **3**

the target protein selectivity, while a molecular modeling study based on the reported crystal structure of the enzyme helps to rationalize the binding modes of these compounds in the active site.

Design and Chemistry

4-Oxo- β -lactams **3a–r** (see Table 1 for a full listing of R¹, R², and R³ substituents) were readily prepared from the appropriate 2,2-disubstituted malonic acid dichlorides, **4**, and amines, as described previously (Scheme 1).³² Compound **3m** was synthesized by reacting ethylbutylketene, generated in situ, with phenyl isocyanate.³⁴ Substituents at C-3 of the 4-oxo- β -lactam scaffold were varied in order to assess the effect of size and lipophilicity on the inhibitor specificity for HLE versus cathepsin G and proteinase-3. Cathepsin G has both chymotrypsin- and trypsin-like specificities, and thus, the specificity of cathepsin G is directed toward substrates with a Phe or a Lys residue at the P₁ position (accommodated at the primary specificity enzyme pocket, S₁),^{8,35–37} while proteinase-3 is more restrictive for the P₁ position than HLE.^{8,38}

Previous studies reporting that substituents at the N-1 position of β -lactam inhibitors interact preferentially with the S₁' subsite of HLE^{23,39} suggested that the *N*-aryl moiety in 4-oxo- β -lactams could be explored as an anchor to probe the interaction with S_n' subsites. The fact that aryl and heterocyclic sulfides had been successfully used as a highly flexible design element in the design of serine protease inhibitors^{40,41} prompted us to design *N*-aryl-4-oxo- β -lactams with a para- or ortho-thioether function, **6** (Scheme 2), as potential mechanism-based inhibitors featuring a latent electrophilic quinone methide imine function upon ring-opening, which upon further reaction with an active site nucleophilic residue (e.g., His-57) would ultimately lead to irreversible inactivation of the enzyme (Scheme 3).⁴¹ Thioether derivatives **6a–j** were synthesized by first converting 4-oxo- β -lactams **3b**, **3f**, and **3h** into their bromomethyl derivatives **5a–c** using NBS and then reacting these with the appropriate thiol in the presence of triethylamine (Scheme 2).

Results and Discussion

Inhibition Kinetics. All 4-oxo- β -lactams **3** and **6** displayed time-dependent inhibition of HLE, and their inhibitory activity was determined using the progress curve method.^{23,27} The progress curves presented an initial exponential phase followed by a linear steady-state turnover of the substrate and were analyzed by the formalism of slow binding kinetics:

$$A = v_s t + (v_i - v_s)[1 - \exp(-k_{\text{obs}}t)]/k_{\text{obs}} + A_0 \quad (1)$$

where *A* is the absorbance at 410 nm (related to the concentration of 4-nitroaniline formed upon hydrolysis of the MeOSuc-Ala-Ala-Pro-Val-*p*-nitroanilide substrate through an extinction coefficient of 8250 M⁻¹ cm⁻¹), *A*₀ is the

absorbance at time *t* = 0, *v*_i and *v*_s are the initial and final rates of product formation, and *k*_{obs} is the pseudo-first-order rate constant for the approach to the steady state.⁴² Such kinetic behavior was reported for other acylating agents of serine proteases, including β -lactams.¹⁹ For the more potent inhibitors, **6e–j**, extremely rapid enzyme inhibition was observed at very low inhibitor concentrations. In these experimental conditions, where the inhibitor concentration was not much higher than that of HLE (i.e., <10[E]), the progress curves had the same shape as those described by eq 1 but were fitted to the more general eq 2.⁴³

$$A = v_s t + [(v_i - v_s)(1 - \gamma)/(k_{\text{obs}}\gamma)] \ln\{[1 - \gamma \exp(-k_{\text{obs}}t)]/(1 - \gamma)\} + A_0 \quad (2)$$

where

$$\gamma = ([E]/[I])[1 - (v_s/v_i)]^2 \quad (3)$$

Typical progress curves for compounds **3h** and **6f** determined at different concentrations are shown in Figure 1.

For most inhibitors (**3a**, **3c**, **3f–q**, **6d–e**, **6h–j**), the pseudo-first-order rate constant for the approach to the steady-state, *k*_{obs}, presented a linear dependence with inhibitor concentration, consistent with the simple time-dependent inhibition via the slow association mechanism A depicted in Scheme 4,⁴² where *k*_{obs} has the relationship

$$k_{\text{obs}} = k_{\text{on}}[I]/(1 + [S]/K_m) + k_{\text{off}} \quad (4)$$

and where *k*_{on} is the second-order rate constant for the formation of the enzyme–inhibitor complex, EI, and *k*_{off} is the first-order rate for the decomposition of EI. The steady-state dissociation constant of the enzyme–inhibitor complex, *K*_i, was calculated using the steady-state velocity, *v*_s, together with *v*_i, and fitting them by nonlinear regression to eq 5,⁴⁴ and *k*_{off} was calculated from eq 6:

$$v_s = \frac{v_0}{[I]/\{K_i(1 + [S]/K_m)\} + 1} \quad (5)$$

$$K_i = k_{\text{off}}/k_{\text{on}} \quad (6)$$

where *v*₀ is the rate for product formation in the absence of inhibitor. As an example, the analysis of inhibition kinetics by 4-oxo- β -lactam **3h** is presented in Figures 2 and 3. For the remaining inhibitors (**3b**, **3d–e**, **6a–c**, **6f,g**), a hyperbolic plot of *k*_{obs} versus [I]/(1 + [S]/K_m) was observed, consistent with a mechanism involving rapid equilibration between the enzyme and inhibitor to form the preassociation complex EI, which then isomerizes relatively slowly to the tight or stable complex, EI* (mechanism B, Scheme 4). Accordingly, *k*_{obs} is given by eq 7

$$k_{\text{obs}} = \frac{k_5[I]}{[K_d(1 + [S]/K_m)] + [I]} + k_6 \quad (7)$$

where *K*_d is the dissociation constant for EI. As an example, the analysis of inhibition kinetics by compound **6f** is presented in Figure 4. The second-order rate constant for the formation of EI*, *k*_{on}, and the dissociation constant for EI*, *K*_i*, were calculated through eqs 8 and 9, respectively:

$$k_{\text{on}} = k_5/K_d \quad (8)$$

$$K_i^* = K_d \left(\frac{k_6}{k_5 + k_6} \right) \quad (9)$$

Table 1. 4-Oxo- β -lactams Prepared and the Corresponding Kinetic Data for HLE Inhibition^c

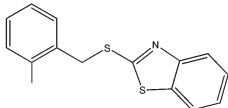
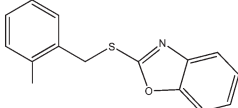
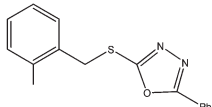
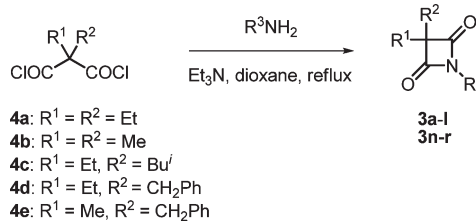
Compd	R ¹	R ²	R ³	$k_{on}/M^{-1}s^{-1}$	k_{off} or k_6/s^{-1}	k_5/s^{-1}	K_i or K_i^*/nM
3a	Et	Et	C ₆ H ₄ -4-OMe	3.05x10 ⁵	2.2x10 ⁻⁴	--	0.71
3b	Et	Et	C ₆ H ₄ -4-Me	6.47x10 ⁵	~0	3.12x10 ⁻²	ND (48.2 ^a)
3c	Et	Et	C ₆ H ₅	2.41x10 ⁵	2.9x10 ⁻⁴	--	1.21
3d	Et	Et	C ₆ H ₄ -4-Cl	6.61x10 ⁵	~0	3.83x10 ⁻²	ND (57.9 ^a)
3e	Et	Et	C ₆ H ₄ -4-CN	5.08x10 ⁵	7.1x10 ⁻⁴	3.23x10 ⁻²	63.5
3f	Et	Et	C ₆ H ₄ -2-Me	1.11x10 ³	2.6x10 ⁻⁴	--	233
3g	Et	Et	pyridin-3'-yl	1.01 x10 ⁵	2.3x10 ⁻⁴	--	2.2
3h	Et	Et	6'-methylpyridin-3'-yl	1.66 x10 ⁵	2.2x10 ⁻⁴	--	1.3
3i	Et	Et	1'-naphthyl	4.35x10 ³	1.5x10 ⁻⁴	--	33.9
3j	Et	Et	CH ₂ Ph	1.76x10 ³	2.0x10 ⁻⁴	--	114
3k	Et	Et	CH ₂ CO ₂ Et	7.33x10 ²	1.6x10 ⁻⁴	--	219
3l	Et	<i>iso</i> -Bu	C ₆ H ₅	2.85x10 ⁴	1.1x10 ⁻⁴	-	3.9
3m	Et	<i>n</i> -Bu	C ₆ H ₅	2.86x10 ⁵	2.4x10 ⁻⁴	--	0.85
3n	Et	CH ₂ Ph	C ₆ H ₅	2.00x10 ³	2.5x10 ⁻⁴	--	127
3o	Me	CH ₂ Ph	C ₆ H ₅	2.67x10 ²	1.2x10 ⁻³	--	4450
3p	Me	Me	CH ₂ Ph	6.21x10 ³	2.1x10 ⁻⁴	--	34.4
3q	Me	Me	C ₆ H ₄ -4-Cl	3.94x10 ⁵	9.4x10 ⁻³	--	23.8
3r	Me	Me	C ₆ H ₅	1.87x10 ⁵ ^b	ND	--	ND
6a	Et	Et		1.50x10 ⁴	1.5x10 ⁻³	4.24x10 ⁻³	99.3 (283 ^a)
6b	Et	Et		3.49x10 ⁴	2.7x10 ⁻⁴	7.15x10 ⁻³	7.6 (205 ^a)
6c	Et	Et		5.99x10 ⁴ ^a	~0	2.12x10 ⁻²	ND (353 ^a)

Table 1. Continued

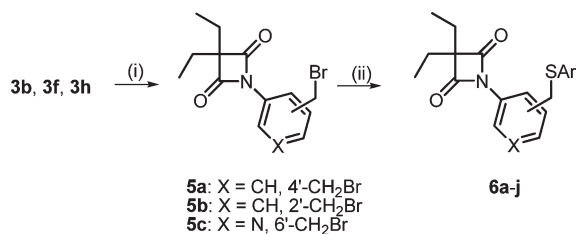
Compd	R ¹	R ²	R ³	$k_{\text{on}}/\text{M}^{-1}\text{s}^{-1}$	k_{off} or k_6/s^{-1}	k_5/s^{-1}	K_i or K_i^*/nM
6d	Et	Et		1.26×10^3	2.6×10^{-4}	--	203
6e	Et	Et		1.15×10^6	9.4×10^{-4}	--	0.82
6f	Et	Et		3.24×10^6	1.2×10^{-3}	9.57×10^{-3}	0.34 (3.0 ^a)
6g	Et	Et		1.77×10^6	2.0×10^{-3}	1.68×10^{-2}	1.0 (9.5 ^a)
6h	Et	Et		2.28×10^6	2.6×10^{-3}	--	1.1
6i	Et	Et		3.18×10^6	1.6×10^{-3}	--	0.50
6j	Et	Et		1.17×10^6	2.1×10^{-3}	--	1.8

^a Value for K_d (see eq 7). ^b $k_{\text{obs}}/[\text{I}]$ determined at $[\mathbf{3r}] = 0.5 \mu\text{M}$. ^c See text for definition of each kinetic parameter.

Scheme 1. Synthesis of 4-Oxo- β -lactams **3a–l** and **3n–r**



Scheme 2. Synthesis of 4-Oxo- β -lactams **6a–j**^a



^a Reagents: (i) NBS, CCl₄; (ii) ArSH, Et₃N, THF.

The relevant kinetic data for the whole set of 4-oxo- β -lactams are outlined in Table 1. The k_{on} values, ranging from 2×10^2 to $3 \times 10^6 \text{ M}^{-1} \text{ s}^{-1}$, were used as an index of inhibitory potency. Remarkably, these association rate constants compare favorably with those of other very potent HLE inhibitors. For example, the k_{on} value for the 4-oxo- β -lactam **6f** is 1 order of magnitude higher than the second-order rate constant for HLE inactivation by β -lactam **2**, (L-680,833, $k_{\text{on}} = 6.22 \times 10^5 \text{ M}^{-1} \text{ s}^{-1}$).²⁶ Modeling studies (see next section) suggest that the tight complex inferred from progress curves resulted from acylation of Ser-195 due to attack on one of the carbonyl carbon atoms of the 4-oxo- β -lactam. In this case, intermediates EI and EI* in mechanisms A and B depicted in Scheme 4, respectively, refer to the acyl-enzyme, and thus, k_6 and k_{off} values reflect the deacylation step. An acylation–deacylation mechanism has been put forward for the reaction of porcine pancreatic elastase with oxo- β -lactams,³² and a similar mechanism has also been reported for other acylating agents of serine proteases.^{44–46} The magnitude of k_{off} and k_6 is very small when compared to k_{obs} and is close to the deacylation rate constants reported for other HLE inhibitors; the value of k_6 for compounds **3b**,

3b, and **6c** could not be distinguished from zero, and thus, the corresponding K_i^* were not determined.

To study the efficiency of inactivation, titration of enzymatic activity studies was performed in which HLE was incubated during 30 min with different concentrations of **3e** at pH 7.2. The fractional remaining activity was found to be proportional to the molar ratio of inhibitor to enzyme, as illustrated in Figure 5. The extrapolation of the line to $v/v_i = 0$ gives the partition ratio; approximately 1.5 molecules of **3e** are required to completely inactivate 1 molecule of enzyme. This result suggests that **3e** is a very efficient irreversible inhibitor of HLE and is consistent with the formation of a tight complex as revealed by the hyperbolic dependence of k_{obs} versus $[I]/(1 + [S]/K_m)$. Similar low partition ratios were also reported for monocyclic β -lactam inhibitors of elastase.²⁷ For example, 1.3 molecules of β -lactam **2** (L-680,833) are required to inactivate HLE to approximately 99%.⁴⁷

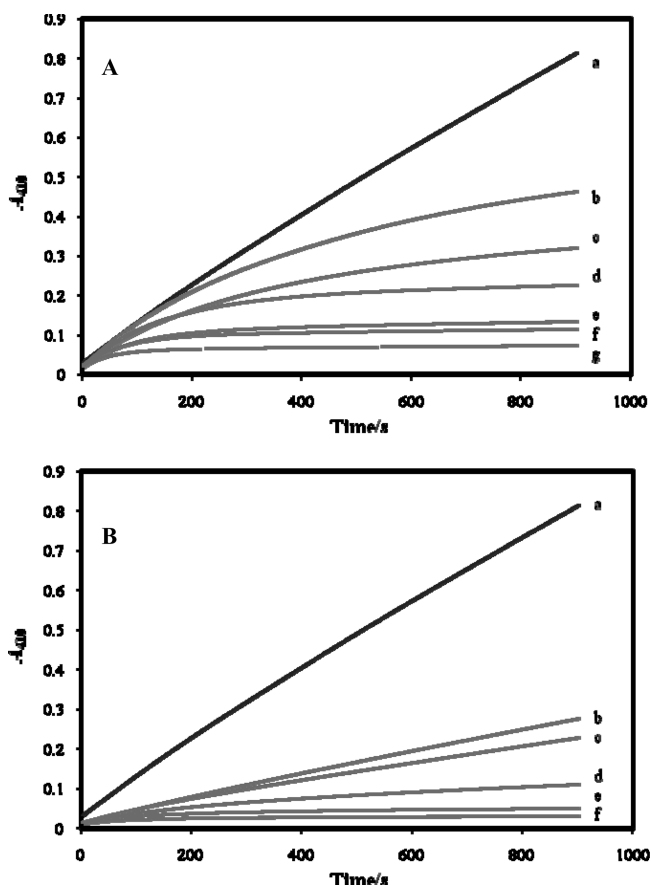
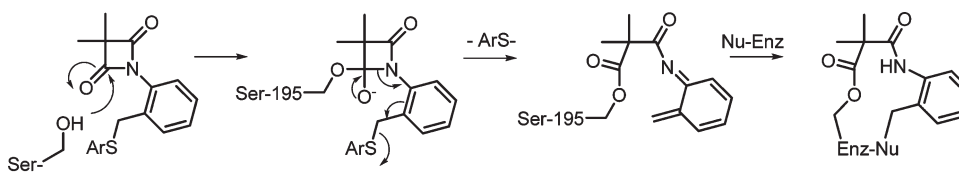


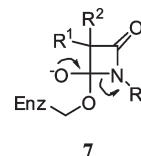
Figure 1. Progress curves for the slow-binding inhibition of HLE by **3h** and **6f**. Reaction conditions are as follows: [HLE] = 20 nM, [MeOSuc-Ala-Ala-Pro-Val-*p*-NA] = 1 mM, 0.1 M HEPES buffer, pH 7.2, 25 °C. Part A shows results for [**3h**]/nM: (a) 0; (b) 75; (c) 100; (d) 250; (e) 375; (f) 500; (g) 750. Part B shows results for [**6f**]/nM: (a) 0; (b) 6.25; (c) 12.5; (d) 25; (e) 50; (f) 75.

Scheme 3. Postulated “Double-Hit” Mechanism for HLE Inactivation by 4-Oxo- β -lactams **6**, Containing a Potential Thiol Leaving Group



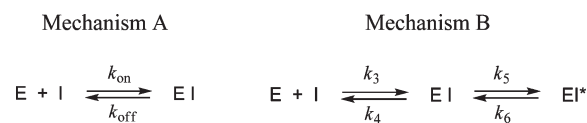
SAR and Modeling Studies. Inspection of the data in Table 1 indicates that inhibitory activity of compounds **3** is strongly dependent on the nature of substituents at C-3 of the 4-oxo- β -lactam ring. For example, replacing one ethyl substituent in **3c** by a larger benzyl moiety, i.e., **3n**, decreased the k_{on} value by 120-fold and increased K_i about 100-fold, while changing the gem-diethyl substitution pattern of **3c** to a methyl benzyl one, i.e., **3o**, decreased the k_{on} value by 900-fold and dramatically increased K_i nearly 3700-fold. In addition, the ethyl isobutyl derivative, **3l**, exhibited only an 8-fold decrease in the k_{on} value when compared to its gem-diethyl counterpart, **3c**. In contrast, the most potent inhibitor in the *N*-phenyl series was the ethyl *n*-butyl derivative, **3m**, with $k_{\text{on}} = 2.9 \times 10^5 \text{ M}^{-1} \text{ s}^{-1}$ and $K_i = 0.85 \text{ nM}$. Overall, these results are consistent with the known preference of HLE for small hydrophobic substituents at C-3 of monocyclic β -lactams for optimal interaction with the S_1 binding pocket of the enzyme.^{23,27}

Derivatives with different *N*-aryl and *N*-alkyl substituents on N-1 were assayed in order to evaluate the effect of the ability of the amide leaving group by C–N bond fission on the inhibitory potency of 3,3-diethyl-4-oxo- β -lactams. Replacing the *N*-benzyl by an *N*-phenyl derivative significantly increases in the rate of enzyme inhibition, as the k_{on} value for **3c** is nearly 137-fold higher than that of **3j**. This effect can be ascribed to the different leaving group abilities of the amide formed from the decomposition of the tetrahedral intermediate **7** generated from **3c** and **3j**. However, the amide leaving group ability is not the only factor affecting inhibitory potency. For example, the *N*-1-naphthyl derivative, **3i**, is 55 times less reactive toward HLE than its *N*-phenyl counterpart, **3c**, suggesting that rigid substituents at this position may be responsible for some nonproductive binding interactions.



The inhibitory potency of 4-oxo- β -lactams **3a–e** toward HLE does not correlate with the Hammett σ_p value of substituents at the aromatic moiety. Analysis of the data for the *N*-aryl, **3a–e**, and *N*-(3'-pyridyl), **3g,h**, series indicates that potency is not significantly affected by the electronic

Scheme 4. Slow-Binding Mechanisms for the Reaction of 4-Oxo- β -lactams with HLE in the Presence of Substrate



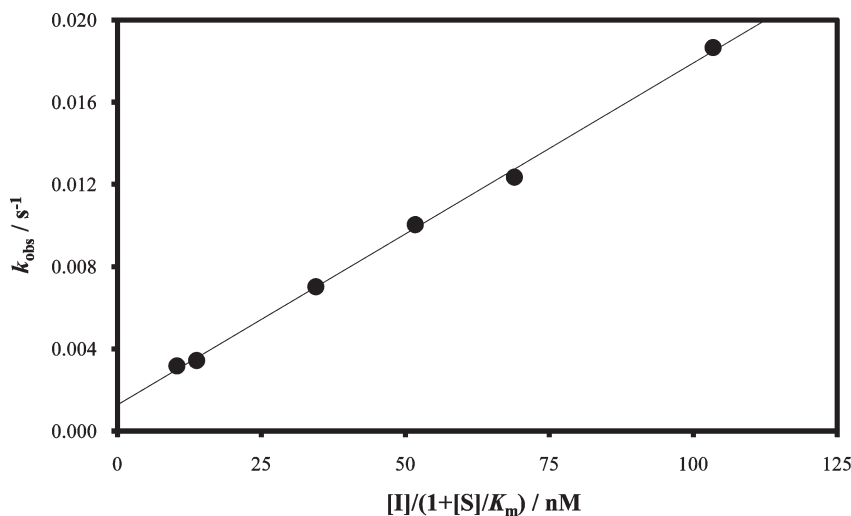


Figure 2. Effect of inhibitor concentration on the onset of inhibition of HLE by **3h**. The values of k_{obs} were obtained as an average of at least duplicate assays from fits to eq 1 of the data shown in Figure 1A.

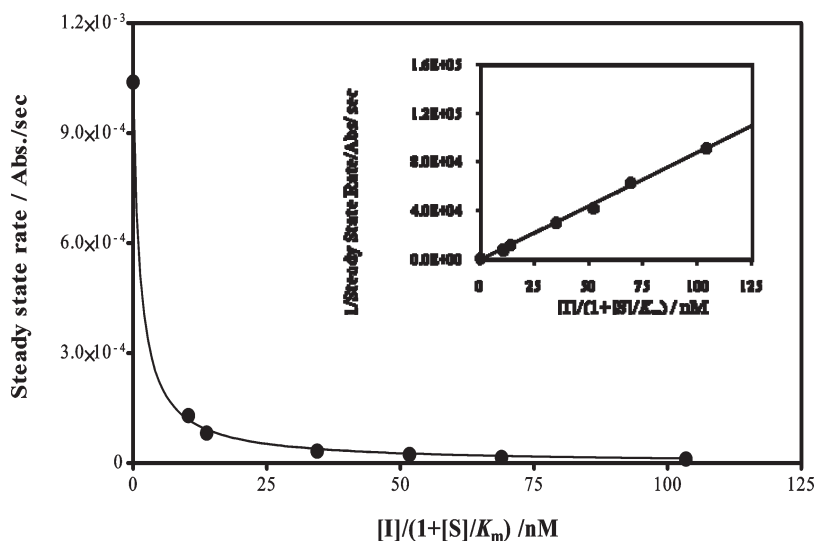


Figure 3. Plot of the steady-state rates versus **[3h]** for the inhibition of HLE. The values for the steady-state rate were obtained from fits to the data shown in Figure 1A. The inset is a Dixon plot to show the linearity.

properties of substituents in the aromatic moiety. For example, the 4-methylphenyl and 4-chlorophenyl derivatives (**3b** and **3d**, respectively) have roughly the same k_{on} values (about $6.5 \times 10^5 \text{ M}^{-1} \text{ s}^{-1}$), which were about 3- and 6-fold higher than those of the unsubstituted and 3'-pyridyl counterparts, **3c** and **3g**, respectively. This can be explained by a significant degree of molecular recognition of these derivatives by HLE. In contrast, previous work showed a good Hammett correlation of the same series of compounds toward PPE,³² indicating that PPE is much more susceptible to intrinsic chemical reactivity effects rather than favorable binding interactions with **3**. Ortho substitution has a detrimental effect on potency, with compound **3b** being 583-fold more potent than **3f**, the ortho positional isomer. This may reflect the less stereochemically hindered carbonyl carbon of **3b** toward nucleophilic attack by Ser-195.

N-Functionalized derivatives that contain a thioether function in the position para to the azetidine ring nitrogen, **6e–j**, present improved inhibitory potency when compared to the unfunctionalized counterparts **3b** and **3h**, with k_{on} values ranging from 1.2×10^6 to $3.2 \times 10^6 \text{ M}^{-1} \text{ s}^{-1}$, and very

low K_i values, ranging from 0.50 to 9.5 nM. These results suggest that the heterocyclic and aryl moieties play an important role in the molecular recognition of **6e–j** by HLE. In contrast, the ortho-substituted derivatives **6a–d** demonstrated inferior levels of inhibitory potency (k_{on}) and much higher K_i values than the corresponding para-analogues, in line with results observed for their unfunctionalized analogues, **3b** and **3f**. Two inhibitors from the para-substituted set, **6f** and **6g**, exhibited a hyperbolic dependence of k_{obs} versus $[I]/(1 + [S]/K_m)$. Since both are derivatives of the thiol 2-mercaptobenzoxazole, we suspect that this moiety allows specific interaction within the active site of the enzyme, thereby facilitating formation of a specific preassociation enzyme–inhibitor complex. Replacing the oxygen atom of the benzoxazole moiety of **6f** by a sulfur atom, giving a benzothiazole moiety (as in **6e**), decreases the inhibitory potency by ~3-fold. This reinforces the idea that the benzoxazole substituent effects a gain in molecular recognition, with its oxygen atom involved in hydrogen bonding within the active site. Interestingly, the incorporation of a meta nitrogen atom into the aromatic ring, as in **6i**, improves inhibitory

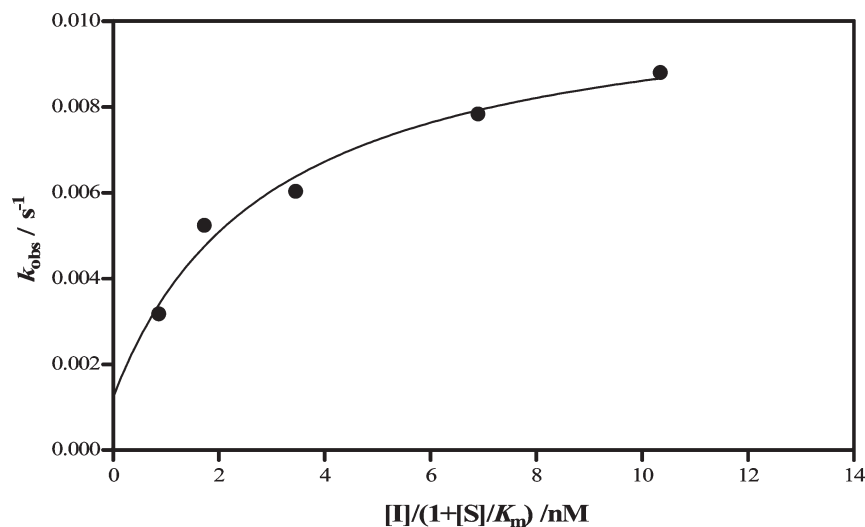


Figure 4. Effect of inhibitor concentration on the onset of inhibition of HLE by **6f**. The values for the steady-state rate were obtained from fits to the data shown in Figure 1B. The solid line was obtained using nonlinear regression analysis to eq 7.

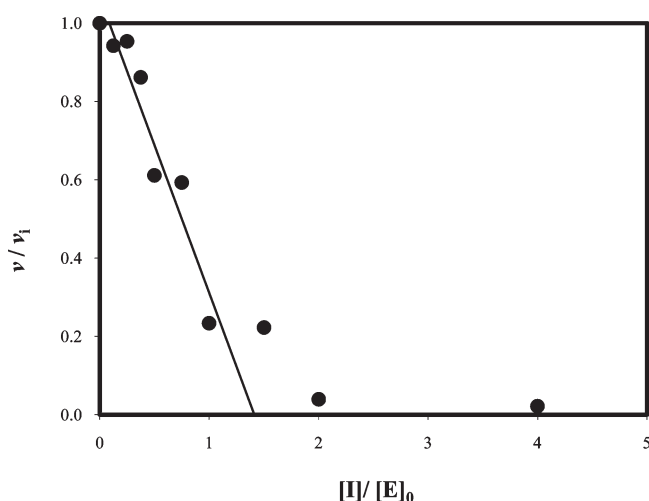


Figure 5. Inactivation of HLE as a function of the ratio $[3e]/[\text{enzyme}]$ at a fixed $[\text{HLE}]$ of $10 \mu\text{M}$. Various amounts of inhibitor **3e** (25–800 nM) in 0.1 M pH 7.2 HEPES buffer were incubated at 25°C for 30 min. Then aliquots were withdrawn and measured for the remaining enzyme activity.

potency when compared to its carba counterpart, **6e**. This finding contrasts with the lower potency of **3g** and **3h**, compared with the corresponding *N*-phenyl analogues.

To obtain a clearer insight into the binding modes between 4-oxo- β -lactams and HLE, we studied the molecular interactions between compounds **3o** (the least potent compound), **6e**, **6f**, and **6i** (the most potent compounds) and the enzyme (PDB code 1HNE) using the program GOLD.⁴⁸ The top 15 conformations (i.e., those with the highest GoldScore fitness score) were visually analyzed for both the hydrophobic interactions between the ligand and the residues defining the S_1 pocket, and the distances between the O_γ oxygen atom of Ser-195 and the two 4-oxo- β -lactam carbonyl carbon atoms ($O_\gamma\text{Ser195}-\text{CO}$). Modeling the interaction of **6e** with HLE revealed that both ethyl substituents at C-3 of the 4-oxo- β -lactam moiety are accommodated in the S_1 pocket where they interact with Val-190, Phe-192, and Val-216 (Figure 6A). Enhanced van der Waals contacts between the benzothiazole moiety with Leu-99 and His-57 were also

observed. The $O_\gamma\text{Ser195}-\text{CO}$ distances for **6e** are 2.6 and 2.8 Å, suggesting that nucleophilic attack by Ser-195 at the 4-oxo- β -lactam is likely to be a facile process. Moreover, the carbonyl of **6e** closest to Ser-195 is involved in the H-bond network of the so-called oxyanion hole defined by the backbone NHs of Gly-193 and Ser-195, suggesting that the oxyanion hole is used to stabilize the tetrahedral intermediate derived from **6e**.

When **6f** and **6i** were docked to HLE, two binding poses were identified: the normal pose (12 and 14 conformations out of the top 15 solutions, respectively), in which the ethyl groups at C-3 of the 4-oxo- β -lactam moiety sit in the S_1 pocket and the carbonyl carbon atoms lie close to the Ser-195 hydroxyl oxygen atom ($O_\gamma\text{Ser195}-\text{CO} = 2.5/2.7$ and $2.5/2.8$ Å, respectively, Figure 6B and Figure 6C); and the inverted pose, in which the benzothiazole (**6i**) and benzoxazole (**6f**) moieties are within the S_1 site, while the four-membered ring is sitting outside the active site. Although the inverted binding mode does not favor HLE acylation (the average shortest $O_\gamma\text{Ser195}-\text{CO}$ distance is 5.3 Å), its low frequency of occurrence is consistent with the observed inhibitory efficiency, as shown by the ~ 3 -fold higher k_{on} values for **6f** and **6i** compared with that for **6e**. The presence of such inverted binding modes in top ranking conformations has been reported for other potent irreversible serine protease inhibitors.⁴⁹ In contrast, all top ranking docking solutions of **3o** correspond to the inverted pose, with the *N*-phenyl group inside the S_1 pocket and an average shortest $O_\gamma\text{Ser195}-\text{CO}$ distance of 5.5 Å (Figure 6D), a result entirely consistent with the weaker HLE inhibition profile of **3o**.

Selectivity Studies. Representative compounds were tested against human neutrophil serine proteases PR3 and cathepsin G and the cysteine protease papain (Table 2). With the exception of **3e** and **3o**, all 4-oxo- β -lactams assayed were found to be time-dependent inhibitors of PR3, although with significantly lower activity in comparison with HLE inhibition. In contrast, most of 4-oxo- β -lactams assayed were inactive or only weakly active against cathepsin G. For example, compound **6f** was $\sim 10^5$ times more potent an inhibitor of HLE than PR3 and was inactive against cathepsin G. A similar selectivity pattern was also observed for **6g** and **6i**. Dual inhibition of HLE and PR3 is not surprising, as it reflects the close similarity of the primary specificity sites of

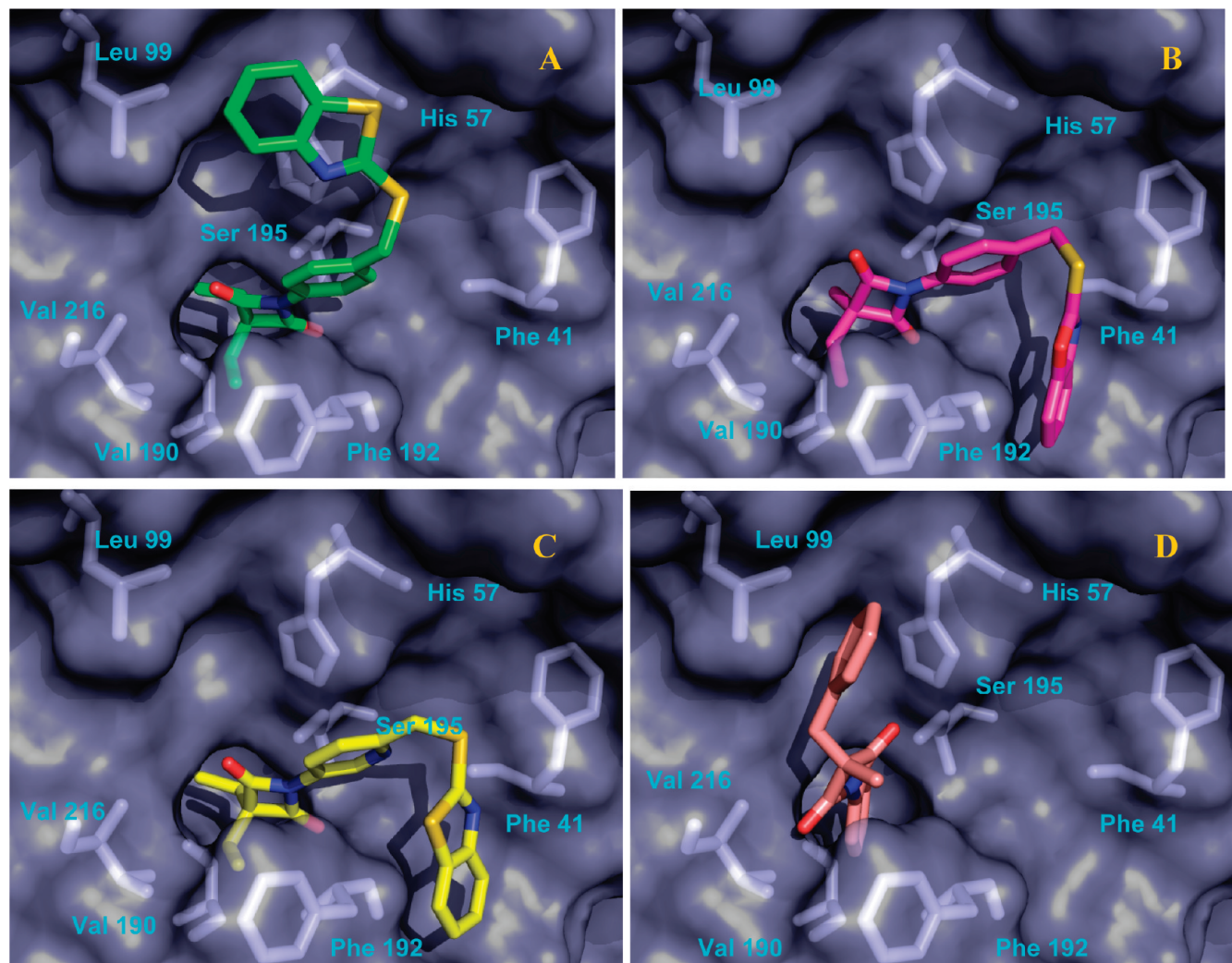


Figure 6. Docking poses of **6e** (A), **6f** (B), **6i** (C), and **3o** (D) in the active site of HLE, obtained from PDB 1HNE. Pictures were prepared using Pymol.⁶⁶

Table 2. Selectivity of Selected 4-Oxo- β -lactams toward HLE, Cathepsin G, Proteinase 3, and Papain^a

compd	k_{on} , $M^{-1}s^{-1}$ HLE	$k_{obs}/[I]$, $M^{-1}s^{-1}$		
		proteinase 3	cathepsin G	papain
3e	5.08×10^5	16% ^b	36.5	NI
3i	4.35×10^3	ND	35.6	NI
3m	2.86×10^5	ND	47.3	NI
3n	2.00×10^3	20.2	NI	NI
3o	2.67×10^2	22% ^c	NI	NI
6b	3.49×10^4	361	NI	NI
6f	3.24×10^6	29.6	NI	NI
6g	1.77×10^6	689	NI	NI
6i	3.18×10^6	4080	NI	NI
6j	1.17×10^6	122	ND	NI

^aNI: no inhibition at 60 μ M. ND: not determined. ^bAt 10 μ M (highest concentration used). ^cAt 60 μ M (highest concentration used).

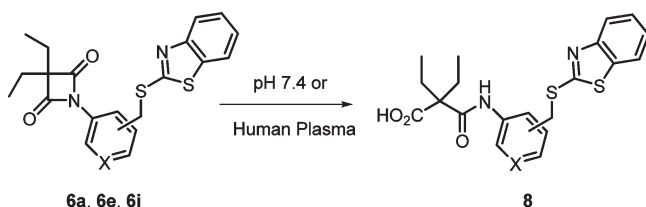
both enzymes⁸ and is consistent with similar observations previously described for other scaffolds.⁴⁰ As both of these neutrophil serine proteases are involved in inflammation and extracellular matrix destruction observed in pulmonary diseases, a potent inhibition of HLE combined with a weaker inhibition of PR3 may be an advantage for therapeutics.

The general lack of cathepsin G inhibition shown by 4-oxo- β -lactams is consistent with the known substrate specificity, since this enzyme has a trypsin and a chymotrypsin-like preference for P₁, accepting aromatic and positively charged side chains.⁸ Surprisingly, neither the methyl benzyl, **3n**, or the ethyl benzyl, **3o**, derivatives inhibit cathepsin G at 60 μ M, despite the presence of an aromatic side chain at P₁. This result may be ascribed to the restricted conformational mobility imparted by the geminal ethyl and methyl groups.

While the *N*-aryl-4-oxo- β -lactams **3a–e** were previously studied against porcine pancreatic elastase (PPE),³² these compounds are much more potent inhibitors of HLE. In fact, the second-order rate constant for HLE inactivation for these compounds ranges from 2.4×10^5 to $6.6 \times 10^5 M^{-1}s^{-1}$, some 3 orders of magnitude larger than those reported for PPE inhibition. This result accords with the S₁ binding pocket of HLE being larger than that of PPE,³³ thereby allowing optimal interaction with the diethyl group at the C-3 of the 4-oxo- β -lactam moiety. Furthermore, the tight preassociation inhibitor–HLE complex observed for compounds **3b**, **3d**, and **3e** (Table 1) contrasts with the simple association mechanism reported for PPE inhibition.³² Finally, all 4-oxo- β -lactams tested were inactive against the cysteine protease, papain, thus suggesting a high degree of

Table 3. Aqueous and Plasma Stability at 37 °C for Compounds **6a**, **6e**, and **6i**

compd	$t_{1/2}$, h	
	buffer, pH 7.4	80% human plasma
6a	37	1.6
6e	10	0.4
6i	13	0.2

Scheme 5. Products for Hydrolysis of **6a**, **6e**, and **6i** in pH 7.4 Buffer and in Human Plasma

selectivity of the azetidine-2,4-dione scaffold toward serine proteases and, in particular, HLE.

Hydrolytic Stability. Stability toward hydrolysis is a prerequisite for maintaining the therapeutically useful concentrations in biological fluids, such as pulmonary epithelial lining fluid and plasma. Thus, the stability of the three compounds containing a benzothiazolylthiomethyl moiety, **6a**, **6e**, and **6i**, was evaluated in pH 7.4 phosphate buffer saline at 37 °C. These were observed to have reasonable stability under physiological conditions, compound **6a** being the most stable with a half-life of 37 h (Table 3). This value is well within the range of hydrolytic half-lives (pH 7.4 and 37 °C) reported for cephalosporin sulfones,^{22,50} *N*-acyl- and *N*-sulfonylazetidin-4-ones,⁵¹ and other β -lactams⁵² but lower than those reported for *N*-carbamoylazetidin-4-ones.⁵³ The product of hydrolysis in all cases was the corresponding *N*-aryl-2,2-diethylpropanedioic acid monoamide **8** (Scheme 5), which implies that departure of the benzothiazolylthiol leaving group is not an efficient process under physiological conditions. This result also suggests that inhibition of HLE by compounds **6** does not involve departure of the leaving group and subsequent formation of an electrophilic quinone methide imine.

In human plasma, compounds **6a**, **6e**, and **6i** were rapidly hydrolyzed, with half-lives ranging from 0.2 to ~2 h. 4-Oxo- β -lactams are thus susceptible to plasma enzymes, in line with the pronounced susceptibility of neutral β -lactam derivatives (e.g., penicillin esters) to undergo plasma-catalyzed hydrolysis of the β -lactam ring.⁵² Overall, these results indicate that although the oral availability of 4-oxo- β -lactams might be limited by compound stability, these inhibitors might be suitable for aerosolization, a route of administration commonly employed for other agents used for lung diseases.⁵⁴ Aerosolization circumvents the problems of absorption and metabolism associated with systemic administration and should also lessen any possible side effects.⁵⁵

Conclusion

4-Oxo- β -lactam HLE inhibitors have been designed to incorporate the structural requirements for optimal interaction at the S_1 primary selectivity pocket of the enzyme. The SAR data indicate that substituents at C-3 of the four-membered ring are a major determinant of the inhibitory

potency. In addition, derivatives containing a benzoxazole- or benzothiazolylthiomethyl group in the *N*-aryl moiety embody a general motif that allows an extremely potent and time-dependent irreversible inhibition of HLE, with some compounds displaying k_{on} values higher than $10^6 \text{ M}^{-1} \text{ s}^{-1}$. Docking studies reveal that ethyl substituents at C-3 of the 4-oxo- β -lactam moiety are well accommodated in the hydrophobic S_1 pocket, allowing proper orientation between the $O\gamma$ oxygen atom of Ser-195 and at least one of the 4-oxo- β -lactam carbonyl carbon atoms. These inhibitors were relatively specific for HLE when compared to proteinase 3 and cathepsin G but displayed absolute specificity when compared to pappain. Some of the most potent and selective inhibitors are relatively stable in pH 7.4 buffer but reactive in 80% human plasma, suggesting that they might be susceptible to esterases. To the best of our knowledge, this is the first comprehensive SAR and selectivity study of 4-oxo- β -lactam HLE inhibitors, which reveals the key structural determinants for inhibitory potency and suggests that the 4-oxo- β -lactam scaffold represents a novel lead for further optimization.

Experimental Section

General. Melting points were determined using a Kofler camera Bock monoscope M and are uncorrected. The infrared spectra were collected on a Nicolet Impact 400 FTIR infrared spectrophotometer and the NMR spectra on a Bruker 400 Ultra-Shield (400 MHz) in CDCl_3 ; chemical shifts, δ , are expressed in ppm, and coupling constants, J , are expressed in Hz. Low-resolution mass spectra were recorded using an HP5988A spectrometer, by RIAIDT, University of Santiago de Compostela, Spain. Compounds were determined to be > 95% pure by elemental analysis (for C, H, and N) performed at Medac Ltd., Brunel Science Centre, Englefield Green, Egham, TW20 0JZ, U.K., or by ITN, Chemistry Unit, Sacavém, Portugal. UV spectra and spectrophotometric assays were recorded using either a Shimadzu UV-1603 or UV-2100 PC spectrophotometer. Thin layer chromatography was performed using Merck silica gel 60 F₂₅₄ aluminum plates and visualized by UV light and/or iodine. Preparative column chromatography was performed using Merck silica gel 60 (70–230 mesh ASTM). Dioxane, tetrahydrofuran, and triethylamine were dried before use. Solvents and buffer materials for enzyme assays were of analytical reagent grade and were purchased from Merck or Sigma. Cathepsin G (EC 3.4.21.20), MeOSuc-Ala-A-Ala-Pro-Val-*p*-NA, and Suc-Ala-Ala-Pro-Phe-*p*-NA were purchased from Sigma, and HLE (EC 3.4.21.37) and proteinase 3 (EC.3.4.21.76) were purchased from Calbiochem. Compounds **3a–e**, **3j–k**, **3m**, **3p–r** were synthesized as described in the literature.^{32,34}

General Procedure for the Synthesis of 4-Oxo- β -lactam Derivatives **3.** The necessary primary amine (0.015 mol) in dioxane (15 mL) was added under a nitrogen atmosphere to a solution of the appropriate malonyl dichloride (0.015 mol) in dioxane (15 mL). A solution of triethylamine (0.036 mol) in dioxane (15 mL) was then added dropwise during 1.5 h and the resulting mixture subsequently refluxed for 6 h, reaction progress being monitored by TLC. After the mixture was cooled, triethylamine hydrochloride was filtered off and the solvent removed under reduced pressure, yielding a solid (the corresponding malon-diamide). The mother liquor was concentrated under reduced pressure and the residue purified by chromatography on silica gel, affording the desired azetidine-2,4-dione.

3,3-Diethyl-1-*o*-tolylazetidine-2,4-dione (3f**).** **3f** was prepared using diethylmalonyl dichloride (0.015 mol) and *o*-toluidine (0.015 mol). The product was purified by chromatography on silica gel using hexane/ethyl acetate (8:2) and subsequently by preparative TLC, yielding the product as a colorless oil (6%). δ

^1H NMR 1.15 (6H, t, $J = 7.6$); 1.90 (4H, q, $J = 7.6$); 2.38 (3H, s); 7.26–7.27 (2H, m); 7.30–7.32 (2H, m); $\delta^{13}\text{C}$ NMR 9.52, 18.83, 24.11, 70.80, 125.59, 126.68, 129.03, 129.83, 131.43, 133.83, 172.84.

3,3-Diethyl-1-(pyridin-3-yl)azetidine-2,4-dione (3g). **3g** was prepared using diethylmalonyl dichloride (0.015 mol) and 3-aminopyridine (0.015 mol). The product was purified by column chromatography on silica gel using dichloromethane/ethyl acetate (9.5:0.5) to give a light-yellow solid, mp 38 °C (47%). $\delta^{13}\text{C}$ NMR 1.10 (6H, t, $J = 7.6$); 1.90 (4H, q, $J = 7.6$); 7.38 (1H, ddd, $J = 8.4, 4.8, 0.4$); 8.35 (1H, ddd, $J = 8.4, 2.8, 1.6$); 8.55 (1H, dd, $J = 4.8, 1.6$); 9.16 (1H, d, $J = 2.8$); $\delta^{13}\text{C}$ NMR 9.22, 23.93, 72.40, 123.84, 126.21, 130.83, 140.77, 147.71, 171.73.

3,3-Diethyl-1-(6-methylpyridin-3-yl)azetidine-2,4-dione (3h). **3h** was prepared as described for **3a**, using diethylmalonyl dichloride (0.0075 mol) and 5-amino-2-methylpyridine (0.0075 mol). The product was purified by column chromatography on silica gel using dichloromethane/ethyl acetate (9.5:0.5) and recrystallized from dichloromethane–hexane to give white crystals (39%), mp 44–45 °C. $\delta^{13}\text{C}$ NMR 1.09 (6H, t, $J = 7.6$); 1.89 (4H, q, $J = 7.6$); 2.59 (3H, s); 7.22 (1H, d, $J = 8.4$); 8.04 (1H, dd, $J = 8.4, 2.4$); 9.01 (1H, d, $J = 2.4$); $\delta^{13}\text{C}$ NMR 9.22, 23.91, 24.25, 72.25, 123.34, 126.74, 129.24, 140.13, 156.83, 171.80.

3,3-Diethyl-1-(naphthalen-1-yl)azetidine-2,4-dione (3i). **3i** was prepared using diethylmalonyl dichloride (0.015 mol) and naphthalen-1-amine (0.015 mol). The product was purified by column chromatography on silica gel using hexane/ethyl acetate (8:2), recrystallized from hexane, to yield a white solid (5%), mp 49–50 °C. $\delta^{13}\text{C}$ NMR 1.26 (6H, t, $J = 7.6$); 2.00 (4H, q, $J = 7.6$); 7.50–7.64 (4H, m); 7.89–7.93 (3H, m); $\delta^{13}\text{C}$ NMR 9.63, 24.25, 71.32, 123.06, 123.32, 125.21, 126.77, 127.17, 127.20, 127.90, 128.47, 129.43, 134.36, 173.26.

3-Ethyl-3-isobutyl-1-phenylazetidine-2,4-dione (3l). **3l** was prepared using 2-ethyl-2-isobutylmalonyl dichloride (0.014 mol) and aniline (0.014 mol). The product was purified by chromatography on silica gel using hexane/ethyl acetate (9:1), yielding the desired product as a colorless oil (12%). $\delta^{13}\text{C}$ NMR 1.00 (6H, d, $J = 6.4$); 1.08 (3H, t, $J = 7.6$); 1.75 (2H, d, $J = 6.4$); 1.81–1.91 (3H, m); 7.29 (1H, dt, $J = 7.6, 1.2$); 7.44 (2H, dt, $J = 7.6, 1.2$); 7.86 (2H, dd, $J = 7.6, 1.2$); $\delta^{13}\text{C}$ NMR 9.09, 23.66, 25.04, 25.26, 39.80, 70.89, 119.20, 126.77, 129.29, 133.93, 172.46.

3-Benzyl-3-ethyl-1-phenylazetidine-2,4-dione (3n). **3n** was prepared using 2-benzyl-2-ethylmalonyl dichloride (0.0081 mol) and aniline (0.0081 mol). The product was purified by chromatography on silica gel using hexane/ethyl acetate (8:2) and recrystallized from hexane, yielding white crystals (22%), mp 76–77 °C. $\delta^{13}\text{C}$ NMR 1.11 (3H, t, $J = 7.6$); 1.95 (2H, q, $J = 7.6$); 3.10 (2H, s); 7.20–7.24 (2H, m); 7.27–7.28 (4H, m); 7.33 (2H, dt, $J = 7.6, 1.2$); 7.52 (2H, dd, $J = 7.6, 1.2$); $\delta^{13}\text{C}$ NMR 9.33, 24.42, 37.38, 73.37, 119.61, 126.90, 127.38, 128.57, 129.11, 129.63, 132.99, 134.86, 171.36.

3-Benzyl-3-methyl-1-phenylazetidine-2,4-dione (3o). **3o** was prepared using 2-benzyl-2-methylmalonyl dichloride (0.016 mol) and aniline (0.016 mol). The product was purified by column chromatography on silica gel using hexane/ethyl acetate (8:2), subsequently by preparative TLC, and recrystallized from dichloromethane–hexane to yield white crystals (5%), mp 54–55 °C. $\delta^{13}\text{C}$ NMR 1.57 (3H, s); 3.10 (2H, s); 7.20–7.24 (2H, m); 7.27–7.29 (4H, m); 7.33 (2H, dt, $J = 7.6, 1.2$); 7.56 (2H, dd, $J = 7.6, 1.2$); $\delta^{13}\text{C}$ NMR 16.27, 38.65, 73.03, 119.48, 126.92, 127.56, 128.60, 129.12, 129.56, 134.86, 136.16, 171.51.

General Procedure for the Synthesis of 4-Oxo- β -lactam Derivatives 6. To a solution of the appropriate ortho or para-methyl substituted 4-oxo- β -lactam (**3b**, **3f**, or **3h**, 0.282 mmol) in tetrachloromethane, *N*-bromosuccinimide (NBS, 0.310 mmol) and benzoyl peroxide (0.0282 mmol) were added, and the reaction mixture was heated under reflux for 12 h with monitoring by TLC. The benzoic acid byproduct was removed by filtration and the solvent was removed under reduced pressure to yield the

corresponding bromomethylarylazetidine-2,4-dione, **5**. Derivatives **6** were prepared by adding triethylamine (2.2 mmol) to a solution of the appropriate bromomethyl derivatives **5a–c** (2 mmol) and thiol (2.2 mmol) in dry THF (5 mL). The mixture was stirred at room temperature for 1–8 h, being monitored by TLC. Upon completion, triethylamine hydrochloride was removed by filtration, the solvent removed under reduced pressure, and the residue purified first by chromatography on silica gel and subsequently by preparative TLC.

1-(2-((Benzo[d]thiazol-2-ylthio)methyl)phenyl)-3,3-diethylazetidine-2,4-dione, 6a. **6a** was prepared as described above using **5a** (0.193 mmol) and 2-mercaptobenzothiazole (0.212 mmol). Elution with dichloromethane–hexane, 7:3, yielded a white solid, mp 73–75 °C (68%). $\delta^{13}\text{C}$ NMR 1.15 (6H, t, $J = 7.6$); 1.93 (4H, q, $J = 7.6$); 4.72 (2H, s); 7–28–7.36 (4H, m); 7.44 (1H, t, $J = 8.0$); 7.67–7.68 (1H, ddd, $J = 8.0, 1.2, 0.4$); 7.75 (1H, d, $J = 8.0$); 7.91 (1H, d, $J = 8.0$); $\delta^{13}\text{C}$ NMR 9.45, 23.98, 34.02, 70.80, 121.02, 121.69, 124.36, 125.98, 126.09, 128.84, 129.25, 129.89, 131.42, 132.06, 135.39, 153.05, 165.42, 172.87.

1-(2-((Benzo[d]oxazol-2-ylthio)methyl)phenyl)-3,3-diethylazetidine-2,4-dione, 6b. **6b** was prepared as described above using **5a** (0.284 mmol) and 2-mercaptobenzoxazole (0.314 mmol) to give a white solid (95%), mp 63–66 °C. $\delta^{13}\text{C}$ NMR 1.17 (6H, t, $J = 7.6$); 1.95 (4H, q, $J = 7.6$); 4.66 (2H, s); 7.28 (1H, dt, $J = 7.6, 1.2$); 7.30 (1H, dt, $J = 7.6, 1.2$); 7.33–7.38 (3H, m); 7.43 (1H, ddd, $J = 7.6, 1.2, 0.4$); 7.62 (1H, ddd, $J = 7.6, 1.2, 0.4$); 7.68–7.71 (1H, m); $\delta^{13}\text{C}$ NMR 9.42, 23.94, 32.92, 70.79, 109.92, 118.62, 123.98, 124.34, 125.88, 128.98, 129.24, 129.88, 131.46, 131.83, 141.83, 151.98, 163.74, 172.85.

1-(2-((5-Phenyl-1,3,4-oxadiazol-2-ylthio)methyl)phenyl)-3,3-diethylazetidine-2,4-dione, 6c. **6c** was prepared as described above, using **5a** (0.177 mmol) and 5-phenyl-1,3,4-oxadiazole-2-thiol (0.194 mmol), and purified using dichloromethane–hexane, 8:2, as eluant to yield white crystals (87%), mp 110–112 °C. $\delta^{13}\text{C}$ NMR 1.18 (6H, t, $J = 7.6$); 1.95 (4H, q, $J = 7.6$); 4.67 (2H, s); 7.35–7.40 (3H, m); 7.48–7.56 (3H, m); 7.71 (1H, dd, $J = 6.0, 2.0$); 7.99 (2H, dd, $J = 8.0, 1.6$); $\delta^{13}\text{C}$ NMR 9.47, 23.99, 33.57, 70.83, 123.50, 125.96, 126.69, 129.05, 129.24, 129.27, 129.96, 131.18, 131.73, 131.83, 163.35, 166.03, 172.74.

1-(2-((1-Methyl-1H-imidazol-2-ylthio)methyl)phenyl)-3,3-diethylazetidine-2,4-dione, 6d. **6d** was prepared as described above, using **5a** (0.169 mmol) and 1-methyl-1H-imidazole-2-thiol (0.186 mmol), and purified using ethyl acetate–acetone, 9:1, as eluant to yield a pale-yellow solid (70%), mp 61–63 °C. $\delta^{13}\text{C}$ NMR 1.17 (6H, t, $J = 7.6$); 1.94 (4H, q, $J = 7.6$); 3.11 (3H, s); 4.22 (2H, s); 6.80 (1H, s); 6.93 (1H, d, $J = 7.6$); 7.10 (1H, s); 7.15 (1H, dt, $J = 7.6, 1.6$); 7.25–7.32 (2H, m); $\delta^{13}\text{C}$ NMR 9.50, 23.95, 33.19, 37.31, 70.68, 122.77, 126.32, 128.60, 128.96, 129.32, 129.42, 130.90, 133.82, 139.92, 172.89.

1-(4-(Benzo[d]thiazol-2-ylthio)methyl)phenyl)-3,3-diethylazetidine-2,4-dione, 6e. **6e** was prepared as described above, using **5b** (0.097 mmol) and 2-mercaptobenzothiazole (0.106 mmol), and purified using dichloromethane–hexane, 7:3, as eluant to yield a white solid (73%), mp 102–104 °C. $\delta^{13}\text{C}$ NMR 1.07 (6H, t, $J = 7.6$); 1.86 (4H, q, $J = 7.6$); 4.60 (2H, s); 7.32 (1H, dt, $J = 7.6, 1.2$); 7.45 (1H, dt, $J = 7.6, 1.2$); 7.53 (2H, d, $J = 8.4$); 7.76 (1H, dd, $J = 7.6, 0.4$); 7.83 (2H, d, $J = 8.4$); 7.92 (1H, dd, $J = 7.6, 0.4$); $\delta^{13}\text{C}$ NMR 9.25, 23.96, 37.07, 72.25, 119.37, 121.06, 121.60, 124.41, 126.13, 130.06, 133.22, 135.08, 135.36, 153.06, 165.77, 172.10.

1-(4-(Benzo[d]oxazol-2-ylthio)methyl)phenyl)-3,3-diethylazetidine-2,4-dione, 6f. **6f** was prepared as described above, using **5b** (0.145 mmol) and 2-mercaptobenzoxazole (0.160 mmol), and purified using dichloromethane–hexane, 7:3, as eluant to yield white crystals (59%), mp 96–98 °C. $\delta^{13}\text{C}$ NMR 1.07 (6H, t, $J = 7.6$); 1.86 (4H, q, $J = 7.6$); 4.57 (2H, s); 7.28 (1H, dt, $J = 7.6, 1.2$); 7.32 (1H, dt, $J = 7.6, 1.2$); 7.47 (1H, d, $J = 7.6$); 7.55 (2H, d, $J = 8.4$); 7.65 (1H, d, $J = 7.6$); 7.84 (2H, d, $J = 8.4$); $\delta^{13}\text{C}$ NMR 9.25, 23.97, 36.02, 72.30, 109.98, 118.50, 119.42, 124.12, 124.44, 130.03, 133.40, 134.63, 141.83, 151.93, 164.05, 172.09.

2-(4-(3,3-Diethyl-2,4-dioxoazetidin-1-yl)benzylthio)benzo[d]oxazole-6-carboxylic acid, 6g. **6g** was prepared as described above, using **5b** (0.225 mmol) and 2-mercaptobenzoxazole-5-carboxylic acid, **9** (0.247 mmol), and triethylamine (0.472 mmol). The reaction mixture was acidified with HCl until pH 2 was obtained and extracted with ethyl acetate. After the mixture was dried and the solvent evaporated off, the residue was purified by column chromatography on silica gel, and subsequently by preparative TLC (elution with ethyl acetate), to yield a yellow solid (24%), mp 166–171 °C. δ ^1H NMR 1.07 (6H, t, $J = 7.6$); 1.87 (4H, q, $J = 7.6$); 4.65 (2H, s); 7.52 (1H, d, $J = 8.8$); 7.56 (2H, d, $J = 8.4$); 7.86 (2H, d, $J = 8.4$); 8.11 (1H, d, $J = 8.8$); 8.41 (1H, s); δ ^{13}C NMR 9.25, 23.97, 36.12, 72.32, 109.88, 119.47, 121.05; 126.78, 130.09, 133.48, 134.35, 135.76, 142.02, 151.52, 166.02, 169.87, 172.09.

1-(4-(5-Phenyl-1,3,4-oxadiazol-2-ylthio)methyl)phenyl)-3,3-diethylazetidine-2,4-dione, 6h. **6h** was prepared as described above, using **5b** (0.290 mmol) and 5-phenyl-1,3,4-oxadiazole-2-thiol (0.319 mmol), and purified using dichloromethane–hexane, 9:1, to yield white crystals (71%), mp 120–122 °C; δ ^1H NMR 1.07 (6H, t, $J = 7.6$); 1.87 (4H, q, $J = 7.6$); 4.53 (2H, s); 7.49–7.54 (3H, m); 7.55 (2H, d, $J = 8.4$); 7.85 (2H, d, $J = 8.4$); 8.01 (2H, dd, $J = 8.4, 1.6$); δ ^{13}C NMR 9.22, 23.97, 36.27, 72.29, 119.49, 123.53, 126.68, 129.06, 130.10, 131.74, 133.34, 134.30, 147.38, 163.50, 172.07.

1-(6-(Benzo[d]thiazol-2-ylthio)methyl)pyridin-3-yl)-3,3-diethylazetidine-2,4-dione, 6i. **6i** was prepared as described above by reaction of **5c** with 2-mercaptobenzothiazole (0.166 mmol) and purified using dichloromethane as eluant to yield a white solid (61%); mp 129–131 °C. δ ^1H NMR 1.08 (6H, t, $J = 7.6$); 1.88 (4H, q, $J = 7.6$); 4.76 (2H, s); 7.33 (1H, dt, $J = 8.4, 1.6$); 7.44 (1H, dt, $J = 8.4, 1.6$); 7.66 (1H, d, $J = 8.4$); 7.77 (1H, dd, $J = 8.4, 0.4$); 7.91 (1H, d, $J = 8.4$); 8.12 (1H, dd, $J = 8.4, 2.4$); 9.11 (1H, d, $J = 2.4$); δ ^{13}C NMR 9.23, 23.94, 38.60, 72.46, 121.09, 121.56, 123.85, 124.42, 126.12, 126.87, 129.72, 135.4, 140.36, 152.99, 154.85, 165.69, 171.61.

3,3-Diethyl-1-(4-(phenylthio)methyl)phenyl)azetidine-2,4-dione, 6j. **6j** was prepared as described above by reaction of **5b** (0.229 mmol) with thiophenol (0.252 mmol) and purified using dichloromethane–hexane, 7:3, to yield a colorless oil (79%). δ ^1H NMR 1.08 (6H, t, $J = 7.6$); 1.86 (4H, q, $J = 7.6$); 4.12 (2H, s); 7.20–7.31 (5H, m); 7.34 (2H, d, $J = 8.4$); 7.77 (2H, d, $J = 8.4$); δ ^{13}C NMR 9.26, 23.95, 38.71, 72.15, 119.24, 126.65, 128.95, 129.61, 130.13, 132.76, 135.72, 136.28, 172.17.

Enzyme Kinetics: Progress Curve Method. Inactivation of HLE was studied at 25 °C by mixing 10 μL of HLE stock solution (2 μM in 0.05 M acetate buffer, pH 5.5) to a solution containing 10 μL of inhibitor in DMSO, 20 μL of the MeOSuc-Ala-Ala-Pro-Val-*p*-nitroanilide substrate (50 mM in DMSO), and 960 μL of 0.1 M pH 7.2 HEPES buffer, and the absorbance was continuously monitored at 410 nm for 20 min. Control assays, in which the inhibitor was omitted, ran linearly. Progress curves were fitted to eqs 1 or 2, depending on the inhibitor concentration relative to that of the enzyme.²⁶ The fitting residuals were typically less than ± 0.001 absorbance units, and typical residual standard deviation for both v_s and k_{obs} was in the range 2–8%. The k_{obs} values calculated from the progress plot were fitted to the slow association or the isomerization mechanisms (Scheme 4) using eqs 3 and 7, respectively. The error associated with K_i was usually $\sim 5\%$ and did not show any relationship to the inhibitory potency. The K_m value of 0.16 mM for the hydrolysis of MeO-Suc-Ala-Ala-Pro-Phe-*p*-NA by HLE was determined as described previously.³⁹

Inactivation of cathepsin G was studied at 25 °C by mixing 100 μL of enzyme stock solution (680 nM in 0.05 M acetate buffer, pH 5.5) with a solution containing 10 μL of inhibitor in DMSO, 20 μL of Suc-Ala-Ala-Pro-Phe-*p*-nitroanilide substrate (42.5 mM in DMSO), and 870 μL of 0.1 M pH 7.5 HEPES buffer, and the absorbance was continuously monitored at 410 nm for 20 min. Control assays, in which

the inhibitor was omitted, ran linearly. Data were treated as described above.

Inactivation of proteinase 3 was studied at 25 °C by mixing 70 μL of enzyme stock solution (325 nM in 0.05 M acetate buffer, pH 6, 150 mM NaCl) with a solution containing 10 μL of inhibitor in DMSO, 75 μL of MeOSuc-Ala-Ala-Pro-Val-*p*-nitroanilide substrate (50 mM in DMSO), and 835 μL of 0.1 M pH 7.2 HEPES buffer, and the absorbance was continuously monitored at 410 nm for 20 000 s. Control assays, in which the inhibitor was omitted, ran linearly. Data were treated as described above.

Enzyme Kinetics: Incubation Method. Papain (1 mg/mL) was activated as described,⁵⁶ and the activated enzyme (300 μL) was incubated at 25 °C with 50 μL of the inhibitor in 650 μL of 50 mM pH 7.0 $\text{K}_2\text{HPO}_4/\text{KH}_2\text{PO}_4$ containing 2.5 mM EDTA. At different times, aliquots (100 μL) were withdrawn and transferred to a cuvette thermostated at 25 °C, containing 100 μL of (*S*)-*N*-benzoylarginine-4-nitroanilide (BAPA) substrate (10 mM in DMSO) and 800 μL of 50 mM $\text{K}_2\text{HPO}_4/\text{KH}_2\text{PO}_4$, pH 7.0, containing 2.5 mM EDTA. The absorbance was monitored during 4 min at 410 nm. Control assays, without the inhibitor, were carried out as described above.⁵⁶

Titration of HLE. An amount of 10 μL of HLE stock solution (20 μM in 0.05 M acetate buffer, pH 5.5) was incubated at 25 °C with different concentrations of **3e** (25–800 nM) in DMSO (10 μL) and 980 μL of 0.1 M HEPES buffer, pH 7.2. After incubation of the reaction mixture for 30 min, a 100 μL aliquot was withdrawn and assayed for remaining enzyme activity, as described previously. The partition ratio was determined from the intercept on the *x*-axis of the linear plot of the remaining activity ($[E]_t/[E]_0$), versus the initial ratio of inhibitor to enzyme ($[I]_0/[E]_0$).

HPLC Analysis. The analytical high-performance liquid chromatography (HPLC) system comprised a Merck Hitachi L-7100 pump with an Shimadzu SPD-6AV UV detector, a manual sample injection module equipped with a 20 μL loop, and a Merck LichroCART 250-4 RP8 (5 μm) column equipped with a Merck Lichrocart precolumn (Merck, Germany). An isocratic solvent system of acetonitrile/water (65:35) was used for compounds **6a**, **6e**, and **6i**. The column effluent was monitored at 225 nm for **6a** and 220 nm for compounds **6e** and **6i**.

Hydrolysis in Buffer Solution. The kinetics of hydrolysis of the compounds was studied using HPLC. Usually, a 15 μL aliquot of a 10^{-2} M stock solution of the compound in DMSO was added to 2.5 mL of thermostated phosphate buffer solution (37 °C). At regular intervals, samples of the reaction mixture were analyzed by HPLC using a mobile phase of acetonitrile/water (the composition of which depended on the compound) and a flow rate of 1.0 mL/min.

Hydrolysis in Human Plasma. Human plasma was obtained from the pooled, heparinized blood of healthy donors and was frozen and stored at -20 °C prior to use. For the hydrolysis experiments, the compounds were incubated at 37 °C in human plasma that had been diluted to 80% (v/v) with pH 7.4 isotonic phosphate buffer. At appropriate intervals, aliquots of 100 μL were added to 200 μL of DMSO to both quench the reaction and precipitate plasma proteins. These samples were centrifuged, and the supernatant was analyzed by HPLC for the presence of initial compound and hydrolysis products.

Molecular Modeling. Geometries of compounds **3o**, **6a**, **6e**, and **6i** were energy-minimized using density functional theory.⁵⁷ These calculations were performed with the B3LYP^{58,59} hybrid functional and the 6-31+G(d,p) basis set implemented in Gaussian 03 software package.⁶⁰ After geometry optimizations, partial charges were included using Amber's antechamber module⁶¹ (included with Chimera software).⁶² The HLE structure (PDB code 1HNE⁶³) was obtained by deletion from the active site of the ligand (MeOSuc-Ala-Ala-Pro-Ala chloromethyl ketone) present in the crystal structure. Hydrogen atoms were added, and the correct protonation state of histidine residues was

assigned according to their surrounding environment. The PPE structure was energy minimized, and charges were added using the Amber united atom force field⁶⁴ implemented in Chimera software.⁶² Molecular docking studies of 4-oxo- β -lactams into the active site of HLE enzyme were performed with the flexible GOLD⁴⁸ docking program using the GoldScore scoring function.⁶⁵ Each ligand was initially energy-minimized and then subjected to 10 000 docking runs (with a population size of 100, 100 000 genetic algorithm operations, 5 islands). The top 15 solutions (i.e., those with the highest fitness score) were visually analyzed for (i) the hydrophobic and hydrophilic interactions between the ligand and enzyme surfaces and (ii) the distance between the Ser-195 hydroxyl oxygen atom and the carbonyl carbon atoms of each 4-oxo- β -lactam.

Acknowledgment. This work was funded by Fundação para a Ciência e Tecnologia (FCT, Portugal) through Project PTDC/QUI/64056/2006. J.M. acknowledges FCT for the Ph. D. Grant SFRH/BD/17534/2004.

Supporting Information Available: Analytical data for compounds **3** and **6**; infrared and mass spectra for compounds **3** and **5**; synthesis of compounds **5** and **9**; complete listing of ref 60. This material is available free of charge via the Internet at <http://pubs.acs.org>.

References

- Calverley, P. M. A.; Walker, P. Chronic Obstructive Pulmonary Disease. *Lancet* **2003**, *362*, 1053–1061.
- Murray, C. J. L.; Lopez, A. D. Alternative Projections of Mortality and Disability by Cause 1990–2020: Global Burden of Disease Study. *Lancet* **1997**, *349*, 1498–1504.
- Rennard, S.; Decramer, M.; Calverley, P. M. A.; Pride, N. B.; Soriano, J. B.; Vermeire, P. A.; Vestbo, J. Impact of COPD in North America and Europe in 2000: Subjects' Perspective of Confronting COPD International Survey. *Eur. Respir. J.* **2002**, *20*, 799–805.
- Barnes, P. J. Chronic Obstructive Pulmonary Disease: A Growing but Neglected Global Epidemic. *PLoS Med.* **2007**, *4*, 779–780.
- Hylkema, M. N.; Sterk, P. J.; de Boer, W. I.; Postma, D. S. Tobacco Use in Relation to COPD and Asthma. *Eur. Respir. J.* **2007**, *29*, 438–445.
- Yoshida, T.; Tuder, R. M. Pathobiology of Cigarette Smoke-Induced Chronic Obstructive Pulmonary Disease. *Physiol. Rev.* **2007**, *87*, 1047–1082.
- Malhotra, S.; Man, S. F. P.; Sin, D. D. Emerging Drugs for the Treatment of Chronic Obstructive Pulmonary Disease. *Exp. Opin. Emerging Drugs* **2006**, *11*, 275–291.
- Korkmaz, B.; Moreau, T.; Gauthier, F. Neutrophil Elastase, Proteinase 3 and Cathepsin G: Physicochemical Properties, Activity and Physiopathological Functions. *Biochimie* **2008**, *90*, 227–242.
- Pham, C. T. N. Neutrophil Serine Proteases Fine-Tune the Inflammatory Response. *Int. J. Biochem. Cell Biol.* **2008**, *40*, 1317–1333.
- Roughley, P. J.; Barrett, A. J. The Degradation of Cartilage Proteoglycans by Tissue Proteinases Proteoglycan Structure and Its Susceptibility to Proteolysis. *Biochem. J.* **1977**, *167*, 629–637.
- Chua, F.; Laurent, G. J. Neutrophil Elastase: Mediator of Extracellular Matrix Destruction and Accumulation. *Proc. Am. Thorac. Soc.* **2006**, *3*, 424–427.
- Pham, C. T. N. Neutrophil Serine Proteases: Specific Regulators of Inflammation. *Nat. Rev. Immunol.* **2006**, *6*, 541–550.
- Lungarella, G.; Cavarra, E.; Lucattelli, M.; Martorana, P. A. The Dual Role of Neutrophil Elastase in Lung Destruction and Repair. *Int. J. Biochem. Cell Biol.* **2008**, *40*, 1287–1296.
- Aboud, R. T.; Vimalanathan, S. Pathogenesis of COPD. Part I. The Role of Protease–Antiprotease Imbalance in Emphysema. *Int. J. Tuberc. Lung Dis.* **2008**, *12*, 361–367.
- Lee, W. L.; Downey, G. Leukocyte Elastase Physiological Functions and Role in Acute Lung Injury. *Am. J. Respir. Crit. Care Med.* **2001**, *164*, 896–904.
- Kelly, E.; Greene, C. M.; McElvaney, N. G. Targeting Neutrophil Elastase in Cystic Fibrosis. *Expert Opin. Ther. Targets* **2008**, *12*, 145–157.
- Henriksen, P. A.; Sallenave, J. Human Neutrophil Elastase: Mediator and Therapeutic Target in Atherosclerosis. *Int. J. Biochem. Cell Biol.* **2008**, *40*, 1095–1100.
- Barnes, P. J. New Treatments for COPD. *Nat. Rev. Drug Discovery* **2002**, *1*, 437–446.
- Abbenante, G.; Fairlie, D. P. Protease Inhibitors in the Clinic. *Med. Chem.* **2005**, *1*, 71–104.
- Chughtai, B.; O'Riordan, T. G. Potential Role of Inhibitors of Neutrophil Elastase in Treating Diseases of the Airway. *J. Aerosol Med.* **2004**, *17*, 289–298.
- Konaklieva, M. I. β -Lactams as Inhibitors of Serine Enzymes. *Curr. Med. Chem.: Anti-Infect. Agents* **2002**, *1*, 215–238.
- Doherty, J. B.; Ashe, B. M.; Argenbright, L. W.; Barker, P. L.; Bonney, R. J.; Chandler, G. O.; Dahlgren, M. E.; Dorn, C. P.; Finke, P. E.; Firestone, R. A.; Fletcher, D.; Hagmann, W. K.; Mumford, R.; Ogrady, L.; Maycock, A. L.; Pisano, J. M.; Shah, S. K.; Thompson, K. R.; Zimmerman, M. Cephalosporin Antibiotics Can Be Modified To Inhibit Human-Leukocyte Elastase. *Nature* **1986**, *322*, 192–194.
- Finke, P. E.; Shah, S. K.; Fletcher, D. S.; Ashe, B. M.; Brause, K. A.; Chandler, G. O.; Dellea, P. S.; Hand, K. M.; Maycock, A. L.; Osinga, D. G.; Underwood, D. J.; Weston, H.; Davies, P.; Doherty, J. B. Orally-Active β -Lactam Inhibitors of Human Leukocyte Elastase. 3. Stereospecific Synthesis and Structure–Activity–Relationships for 3,3-Dialkylazetidino-2-ones. *J. Med. Chem.* **1995**, *38*, 2449–2462.
- Firestone, R. A.; Barker, P. L.; Pisano, J. M.; Ashe, B. M.; Dahlgren, M. E. Monocyclic Beta-Lactam Inhibitors of Human-Leukocyte Elastase. *Tetrahedron* **1990**, *46*, 2255–2262.
- Clemente, A.; Domingos, A.; Grancho, A. P.; Iley, J.; Moreira, R.; Neres, J.; Palma, N.; Santana, A. B.; Valente, E. Design, Synthesis and Stability of *N*-Acylloxymethyl- and *N*-Aminocarbonyloxymethyl-2-azetidino-2-ones as Human Leukocyte Elastase Inhibitors. *Bioorg. Med. Chem. Lett.* **2001**, *11*, 1065–1068.
- Doherty, J. B.; Shah, S. K.; Finke, P. E.; Dorn, C. P., Jr.; Hagmann, W. K.; Hale, J. J.; Kissinger, A. L.; Thompson, K. R.; Brause, K.; Chandler, G. O.; Knight, W. B.; Maycock, A. L.; Ashe, B. M.; Weston, H.; Gale, P.; Mumford, R. A.; Andersen, O. F.; Williams, H. R.; Nolan, T. E.; Frankenfield, D. L.; Underwood, D.; Vyas, K. P.; Kari, P. H.; Dahlgren, M. E.; Mao, J.; Fletcher, D. S.; Dellea, P. S.; Hand, K. M.; Osinga, D. G.; Peterson, L. B.; Williams, D. T.; Metzger, J. M.; Bonney, R. J.; Humes, J. L.; Pacholok, S. P.; Hanlon, W. A.; Opas, E.; Stolk, J.; Davies, P. Chemical, Biochemical, Pharmacokinetic, and Biological Properties of L-680,833: A Potent, Orally Active Monocyclic β -Lactam Inhibitor of Human Polymorphonuclear Leukocyte elastase. *Proc. Nat. Acad. Sci. U.S.A.* **1993**, *90*, 8727–8731.
- Mulchande, J.; Martins, L.; Moreira, R.; Archer, M.; Oliveira, T. F.; Iley, J. The Efficiency of C-4 Substituents in Activating the β -Lactam Scaffold towards Serine Proteases and Hydroxide Ion. *Org. Biomol. Chem.* **2007**, *5*, 2617–2626.
- Cainelli, G.; Galletti, P.; Garbisa, S.; Giacomini, D.; Sartor, L.; Quintavalla, A. 4-Alkylidene-azetidino-2-ones: Novel Inhibitors of Leukocyte Elastase and Gelatinase. *Bioorg. Med. Chem.* **2003**, *11*, 5391–5399.
- Wakselman, M.; Joyeau, R.; Kobaiter, R.; Boggetto, N.; Vergely, I.; Maillard, J.; Okochi, V.; Montagne, J. J.; Reboudraux, M. Functionalized *N*-Aryl Azetidino-2-ones as Novel Mechanism-Based Inhibitors of Neutrophil Elastase. *FEBS Lett.* **1991**, *282*, 377–381.
- Sykes, N. O.; Macdonald, S. J. F.; Page, M. I. Acylating Agents as Enzyme Inhibitors and Understanding Their Reactivity for Drug Design. *J. Med. Chem.* **2002**, *45*, 2850–2856.
- Imming, P.; Klar, B.; Dix, D. Hydrolytic Stability versus Ring Size in Lactams: Implications for the Development of Lactam Antibiotics and Other Serine Protease Inhibitors. *J. Med. Chem.* **2000**, *43*, 4328–4331.
- Mulchande, J.; Guedes, R. C.; Tsang, W. Y.; Page, M. I.; Moreira, R.; Iley, J. Azetidino-2,4-diones (4-Oxo- β -lactams) as Scaffolds for Designing Elastase Inhibitors. *J. Med. Chem.* **2008**, *51*, 1783–1790.
- Bode, W.; Meyer, E.; Powers, J. C. Human-Leukocyte and Porcine Pancreatic Elastase: X-ray Crystal-Structures, Mechanism, Substrate-Specificity, and Mechanism-Based Inhibitors. *Biochemistry* **1989**, *28*, 1951–1963.
- Dai, S. A.; Juang, T.; Chen, C.; Chang, H.; Kuo, W.; Suo, W.; Jeng, R. Synthesis of *N*-Aryl Azetidino-2,4-diones and Polymalonamides Prepared from Selective Ring-Opening Reactions. *J. Appl. Polym. Sci.* **2007**, *103*, 3591–3599.
- Powers, J. C.; Tanaka, T.; Harper, J. W.; Minematsu, Y.; Barker, L.; Lincoln, D.; Crumley, K. V.; Fraki, J. E.; Schechter, N. M.; Lazarus, G. G.; Nakajima, K.; Nakashino, K.; Neurath, H.; Woodbury, R. G. Mammalian Chymotrypsin-Like Enzymes: Comparative Reactivities of Rat Mast-Cell Proteases, Human

- and Dog Skin Chymases, and Human Cathepsin-G with Peptide 4-Nitroanilide Substrates and with Peptide Chloromethyl Ketone and Sulfonyl Fluoride Inhibitors. *Biochemistry* **1985**, *24*, 2048–2058.
- (36) Polanowska, J.; Krokoszynska, I.; Czapinska, H.; Watorek, W.; Dadlez, M.; Otlewski, J. Specificity of Human Cathepsin G. *Biochim. Biophys. Acta* **1998**, *1386*, 189–198.
- (37) Rehault, S.; Brillard-Bourdet, M.; Juliano, M. A.; Juliano, L.; Gauthier, F.; Moreau, T. New, Sensitive Fluorogenic Substrates for Human Cathepsin G Based on the Sequence of Serpin-Reactive Site Loops. *J. Biol. Chem.* **1999**, *274*, 13810–13817.
- (38) Kam, C. M.; Kerrigan, J. E.; Dolman, K. M.; Goldschmeding, R.; Vondemborne, A.; Powers, J. C. Substrate and Inhibitor Studies on Proteinase-3. *FEBS Lett.* **1992**, *297*, 119–123.
- (39) Moreira, R.; Santana, A. B.; Iley, J.; Neres, J.; Douglas, K. T.; Horton, P. N.; Hursthouse, M. B. Design, Synthesis, and Enzymatic Evaluation of N^1 -Acloxyalkyl- and N^1 -Oxazolidin-2,4-dion-5-yl-substituted β -Lactams as Novel Inhibitors of Human Leukocyte Elastase. *J. Med. Chem.* **2005**, *48*, 4861–4870.
- (40) He, S.; Kuang, R. Z.; Venkataraman, R.; Tu, J.; Truong, T. M.; Chan, H. K.; Groutas, W. C. Potent Inhibition of Serine Proteases by Heterocyclic Sulfide Derivatives of 1,2,5-Thiadiazolidin-3-one 1,1-Dioxide. *Bioorg. Med. Chem.* **2000**, *8*, 1713–1717.
- (41) Li, Y.; Dou, D. F.; He, G. J.; Lushington, G. H.; Groutas, W. C. Mechanism-Based Inhibitors of Serine Proteases with High Selectivity through Optimization of S' Subsite Binding. *Bioorg. Med. Chem.* **2009**, *17*, 3536–3542.
- (42) Morrison, J. F.; Walsh, C. T. The Behavior and Significance of Slow-Binding Enzyme Inhibitors. *Adv. Enzymol.* **1988**, *61*, 201–301.
- (43) Copeland, R. A. *Evaluation of Enzyme Inhibitors in Drug Discovery: A Guide for Medicinal Chemists and Pharmacologists*; John Wiley and Sons: Hoboken, NJ, 2005; p 296.
- (44) Gutschow, M.; Neumann, U. Novel Thieno[2,3-d][1,3]oxazin-4-ones as Inhibitors of Human Leukocyte Elastase. *J. Med. Chem.* **1998**, *41*, 1729–1740.
- (45) Stein, R. L.; Strimpler, A. M.; Viscarello, B. R.; Wildonger, R. A.; Mauger, R. C.; Trainor, D. A. Mechanism of Slow-Binding Inhibition of Human Leukocyte Elastase by Valine-Derived Benzoxazinones. *Biochemistry* **1987**, *26*, 4126–4130.
- (46) Gutschow, M.; Neumann, U. Inhibition of Cathepsin G by 4H-3,1-Benzoxazin-4-ones. *Bioorg. Med. Chem.* **1997**, *5*, 1935–1942.
- (47) Chabin, R.; Green, B. G.; Gale, P.; Maycock, A. L.; Weston, H.; Dorn, C. P.; Finke, P. E.; Hagmann, W. K.; Hale, J. J.; Maccoss, M.; Shah, S. K.; Underwood, D.; Doherty, J. B.; Knight, W. B. Mechanism of Inhibition of Human-Leukocyte Elastase by Monocyclic β -Lactams. *Biochemistry* **1993**, *32*, 8970–8980.
- (48) CCDC Software Ltd., Cambridge, U.K.
- (49) Frederick, R.; Robert, S.; Charlier, C.; Wouters, J.; Masereel, B.; Pochet, L. Mechanism-Based Thrombin Inhibitors: Design, Synthesis, And Molecular Docking of a New Selective 2-Oxo-2H-1-benzopyran Derivative. *J. Med. Chem.* **2007**, *50*, 3645–3650.
- (50) Alpegiani, M.; Bissolino, P.; Corigli, R.; Delnero, S.; Perrone, E.; Rizzo, V.; Sacchi, N.; Cassinelli, G.; Franceschi, G.; Baici, A. Cephem Sulfones as Inactivators of Human-Leukocyte Elastase. 5. 7-Alpha-methoxy-1,1-dioxocephem-4-ketone and 7-Alpha-chloro-1,1-dioxocephem-4-ketone. *J. Med. Chem.* **1994**, *37*, 4003–4019.
- (51) Sutton, J. C.; Bolton, S. A.; Hartl, K. S.; Huang, M. H.; Jacobs, G.; Meng, W.; Ogletree, M. L.; Pi, Z. L.; Schumacher, W. A.; Seiler, S. M.; Slusarchyk, W. A.; Treuner, U.; Zahler, R.; Zhao, G. H.; Bisacchi, G. S. Synthesis and SAR of 4-Carboxy-2-azetidinone Mechanism-Based Tryptase Inhibitors. *Bioorg. Med. Chem. Lett.* **2002**, *12*, 3229–3233.
- (52) Nielsen, N. M.; Bundgaard, H. Facile Plasma-Catalysed Degradation of Penicillin Alkyl Esters but with No Liberation of the Parent Penicillin. *J. Pharm. Pharmacol.* **1988**, *40*, 506–509.
- (53) Knight, W. B.; Green, B. G.; Chabin, R. M.; Gale, P.; Maycock, A. L.; Weston, H.; Kuo, D. W.; Westler, W. M.; Dorn, C. P.; Finke, P. E.; Hagmann, W. K.; Hale, J. J.; Liesch, J.; MacCoss, M.; Navia, M. A.; Shah, S. K.; Underwood, D.; Doherty, J. B. Specificity, Stability, and Potency of Monocyclic β -Lactam Inhibitors of Human Leukocyte Elastase. *Biochemistry* **1992**, *31*, 8160–8170.
- (54) Finke, P. E.; Shah, S. K.; Ashe, B. M.; Ball, R. G.; Blacklock, T. J.; Bonney, R. J.; Brause, K. A.; Chandler, G. O.; Cotton, M.; Davies, P.; Dellea, P. S.; Dorn, C. P.; Fletcher, D. S.; Ogrady, L. A.; Hagmann, W. K.; Hand, K. M.; Knight, W. B.; Maycock, A. L.; Mumford, R. A.; Osinga, D. G.; Sohar, P.; Thompson, K. R.; Weston, H.; Doherty, J. B. Inhibition of Human-Leukocyte Elastase. 4. Selection of a Substituted Cephalosporin (L-658,758) as a Topical Aerosol. *J. Med. Chem.* **1992**, *35*, 3731–3744.
- (55) Travis, J.; Fritz, H. Potential Problems in Designing Elastase Inhibitors for Therapy. *Am. Rev. Respir. Dis.* **1991**, *143*, 1412–1415.
- (56) Valente, C.; Moreira, R.; Guedes, R. C.; Iley, J.; Douglas, K. T. The 1,4-Naphthoquinone Scaffold in the Design of Cysteine Protease Inhibitors. *Bioorg. Med. Chem.* **2007**, *15*, 5340–5350.
- (57) Parr, R. G.; Yang, W. *Density Functional Theory of the Electronic Structure of Molecules*; Oxford University Press: Oxford, U.K., 1989.
- (58) Becke, A. D. Density Functional Thermochemistry 3. The Role of Exact Exchange. *J. Chem. Phys.* **1993**, *98*, 5648–5652.
- (59) Lee, C. T.; Yang, W. T.; Parr, R. G. Development of the Colle-Salvetti Correlation-Energy Formula into a Functional of the Electron-Density. *Phys. Rev. B* **1988**, *37*, 785–789.
- (60) Frisch, M. J.; Trucks, G. W.; Schlegel, H. B.; Scuseria, G. E.; Robb, M. A.; Cheeseman, J. R.; Montgomery, J. A., Jr.; Vreven, T.; Kudin, K. N.; Burant, J. C.; Millam, J. M.; Iyengar, S. S.; Tomasi, J.; Barone, V.; Mennucci, B.; Cossi, M.; Scalmani, G.; Rega, N.; Petersson, G. A.; Nakatsuji, H.; Hada, M.; Ehara, M.; Toyota, K.; Fukuda, R.; Hasegawa, J.; Ishida, M.; Nakajima, T.; Honda, Y.; Kitao, O.; Nakai, H.; Klene, M.; Li, X.; Knox, J. E.; Hratchian, H. P.; Cross, J. B.; Bakken, V.; Adamo, C.; Jaramillo, J.; Gomperts, R.; Stratmann, R. E.; Yazyev, O.; Austin, A. J.; Cammi, R.; Pomelli, C.; Ochterski, J. W.; Ayala, P. Y.; Morokuma, K.; Voth, G. A.; Salvador, P.; Dannenberg, J. J.; Zakrzewski, V. G.; Dapprich, S.; Daniels, A. D.; Strain, M. C.; Farkas, O.; Malick, D. K.; Rabuck, A. D.; Raghavachari, K.; Foresman, J. B.; Ortiz, J. V.; Cui, Q.; Baboul, A. G.; Clifford, S.; Cioslowski, J.; Stefanov, B. B.; Liu, G.; Liashenko, A.; Piskorz, P.; Komaromi, I.; Martin, R. L.; Fox, D. J.; Keith, T.; Al-Laham, M. A.; Peng, C. Y.; Nanayakkara, A.; Challacombe, M.; Gill, P. M. W.; Johnson, B.; Chen, W.; Wong, M. W.; Gonzalez, C.; Pople, J. A. *Gaussian 03*, revision C.02; Gaussian, Inc.: Wallingford, CT, 2004.
- (61) Wang, J. M.; Wang, W.; Kollman, P. A.; Case, D. A. Automatic Atom Type and Bond Type Perception in Molecular Mechanical Calculations. *J. Mol. Graph. Modell.* **2006**, *25*, 247–260.
- (62) Pettersen, E. F.; Goddard, T. D.; Huang, C. C.; Couch, G. S.; Greenblatt, D. M.; Meng, E. C.; Ferrin, T. E. UCSF Chimera. A Visualization System for Exploratory Research and Analysis. *J. Comput. Chem.* **2004**, *25*, 1605–1612.
- (63) Navia, M. A.; McKeever, B. M.; Springer, J. P.; Lin, T.; Williams, H. R.; Fluder, E. M.; Dorn, C. P.; Hoogsteen, K. Structure of Human Neutrophil Elastase in Complex with a Peptide Chloromethyl Ketone Inhibitor at 1.84-Å Resolution. *Proc. Nat. Acad. Sci. U.S.A.* **1989**, *86*, 7–11.
- (64) Cornell, W. D.; Cieplak, P.; Bayly, C. I.; Gould, I. R.; Merz, K. M.; Ferguson, D. M.; Spellmeyer, D. C.; Fox, T.; Caldwell, J. W.; Kollman, P. A. A 2nd Generation Force-Field for the Simulation of Proteins, Nucleic-Acids, and Organic-Molecules. *J. Am. Chem. Soc.* **1995**, *117*, 5179–5197.
- (65) Jones, G.; Willett, P.; Glen, R. C.; Leach, A. R.; Taylor, R. Development and Validation of a Genetic Algorithm for Flexible Docking. *J. Mol. Biol.* **1997**, *267*, 727–748.
- (66) DeLano, W. L. *The PyMOL Molecular Graphics System*; DeLano Scientific: San Carlos, CA, 2002.